

GNAS 메틸화 이상으로 인한 거짓부갑상선기능저하증 Ib 1예

A Case of Pseudohypoparathyroidism Type Ib Caused by Aberrant Methylation in the GNAS Complex Locus

조성진¹ · 한은희¹ · 장우리¹ · 채효진¹ · 김용구¹ · 이건동¹ · 조원경² · 서병규² · 김명신¹

Sung Jin Jo, M.D.¹, Eunhee Han, M.D.¹, Woori Jang, M.D.¹, Hyojin Chae, M.D.¹, Yonggoo Kim, M.D.¹, Gun Dong Lee, M.T.¹, Won Kyoung Cho, M.D.², Byung-Kyu Suh, M.D.², Myungshin Kim, M.D.¹

가톨릭대학교 의과대학 진단검사의학과¹, 소아청소년과²

Departments of Laboratory Medicine¹ and Pediatrics², College of Medicine, The Catholic University of Korea, Seoul, Korea

Pseudohypoparathyroidism (PHP) is a rare disorder caused by genetic and epigenetic aberrations in the *GNAS* complex locus resulting in impaired expression of stimulatory G protein (Gs α). PHP type Ib (PHP-Ib) is characterized by hypocalcemia and hyperphosphatemia due to renal resistance to the parathyroid hormone, and is distinguished from PHP-Ia by the absence of osteodystrophic features. An 11-yr-old boy presented with poor oral intake and cramping lower limb pain after physical activity. Laboratory studies revealed hypocalcemia, hyperphosphatemia, and increased parathyroid hormone levels. The *GNAS* complex locus was evaluated using the methylation-specific multiplex ligation-dependent probe amplification (MS-MLPA) assay. Gain of methylation in the NESP55 domain and loss of methylation in the antisense (AS) transcript, XL, and A/B domains in the maternal allele were observed. Consequently, we present a case of PHP-Ib diagnosed using MS-MLPA.

Key Words: Pseudohypoparathyroidism, Methylation, *GNAS* complex locus, MLPA

INTRODUCTION

Pseudohypoparathyroidism (PHP) is characterized by peripheral parathyroid hormone (PTH) resistance along with hypocalce-

mia and hyperphosphatemia [1]. The identification of the PTH receptor and its signal transduction pathway facilitated better understanding of PHP pathophysiology. PHP types I and II are distinguished by cyclic AMP (cAMP) levels in response to exogenous PTH [2]. The main PHP subtypes, Ia and Ib (PHP-Ia and PHP-Ib, respectively), are caused by genetic and/or epigenetic alterations within or upstream of the *GNAS* locus. Most patients with PHP-Ia exhibit Albright's hereditary osteodystrophy (AHO) and multi-hormone resistance, while 2/3 of patients with PHP-Ib exhibit only PTH resistance [1]. PHP exemplifies a quite unusual form of hormone resistance as the molecular cause is not a deficiency of the hormone receptor itself, but instead is a partial deficiency of the α -subunit of the stimulatory G protein (Gs α), encoded by the *GNAS* imprinted locus (MIM#139320), a key regulator of the hormone-activated cAMP signaling pathway. The *GNAS* complex locus has multiple promoters and differentially methylated regions (DMRs) and produces several parent-of-origin products [3]. Using parent-specific methylation patterns in the DMRs, the *GNAS* complex produces stimulatory G protein, neuroendocrine secretory pro-

Corresponding author: Myungshin Kim

Department of Laboratory Medicine, College of Medicine, The Catholic University of Korea, Seoul St. Mary's Hospital, 222 Banpo-daero, Seocho-gu, Seoul 06591, Korea

Tel: +82-2-2258-1645, Fax: +82-2-2258-1719, E-mail: microkim@catholic.ac.kr

Co-corresponding author: Byung-Kyu Suh

Department of Pediatrics, College of Medicine, The Catholic University of Korea, Seoul St. Mary's Hospital, 222 Banpo-daero, Seocho-gu, Seoul 06591, Korea

Tel: +82-2-2258-6185, Fax: +82-2-537-4544, E-mail: suhbk@catholic.ac.kr

Received: June 13, 2016

Revision received: August 17, 2016

Accepted: August 18, 2016

This article is available from <http://www.labmedonline.org>

© 2017, Laboratory Medicine Online

© This is an Open Access article distributed under the terms of the Creative Commons Attribution Non-Commercial License (<http://creativecommons.org/licenses/by-nc/4.0/>) which permits unrestricted non-commercial use, distribution, and reproduction in any medium, provided the original work is properly cited.

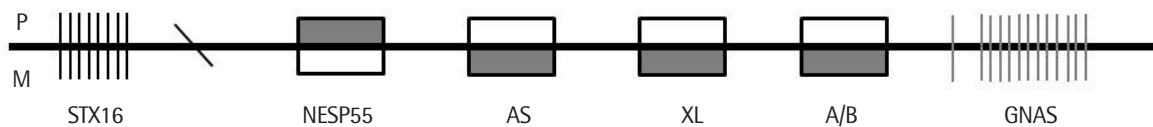


Fig. 1. Multiple methylated regions and *GNAS* gene of the *GNAS* complex locus. The general organization and imprinting patterns of *GNAS* alleles are shown. NESP55 is imprinted in the paternal allele and AS, XL and A/B are imprinted in the maternal allele (grey colored box ■).

tein 55 (NESP55), the extra-large variant of $Gs\alpha$ (XL α s), A/B transcript, and the *GNAS* antisense (AS) transcript (Fig. 1) [3]. PHP-Ia is mainly caused by inactivation of maternally inherited mutations affecting $Gs\alpha$ coding exons. Loss of imprinting in the exon A/B DMR due to microdeletions in *STX16* is the most frequent mechanism of familial PHP-Ib [4-8], while the most sporadic cases of PHP-Ib are caused by imprinting abnormalities of DMRs in the *GNAS* complex [4, 9, 10]; however, no clinical difference was observed between the familial and sporadic forms of PHP-Ib [11]. Endocrine levels and other blood biochemical parameters vary according to the stage of life and disease severity [1]. Although patients with PHP-Ia typically express AHO features, physical features, as well as biochemical and molecular findings in some cases are too ambiguous to distinguish it from PHP-Ib. The long-term effects of elevated PTH levels on the bones are also unclear [1] because various skeletal phenotypes have been observed [12-15]. Therefore, identification of the molecular cause of PHP aids in confirmation of the diagnosis and the understanding of clinical characteristics. In this report, we present a patient with PHP-Ib caused by impaired imprinting in the *GNAS* complex.

CASE

1. Patient

An 11-yr-old boy presented with poor oral intake and cramping pain in both the lower limbs after physical activity. The parents expressed concern that the patient had a slight physique compared to other children in the same age group. However, the patient showed a normal growth rate according to the Korean growth chart (height =142.6 cm, 25-50th percentile, SDS -0.49; body weight =34.7 kg, 10-25th percentile, SDS -0.78). The patient had no family history of any relevant diseases. The patient's blood biochemical investigations revealed hypocalcemia (6.6 mg/dL, reference range 8.0-10.0 mg/dL) and hyperphosphatemia (7.6 mg/dL, reference range 2.6-4.5 mg/dL) with an elevated PTH level (127 pg/mL, reference range 13-54 pg/mL). Thyroid stimulating hormone (TSH) level was in-

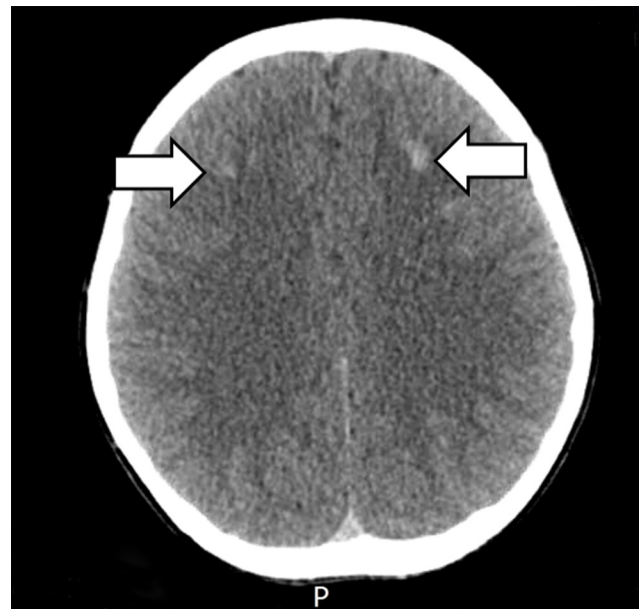


Fig. 2. The brain CT scan. Multiple high density nodular lesions in the bilateral basal ganglia and subcortical white matter of the frontal lobe.

creased (8.42 mIU/L, reference range 0.17-4.05 mIU/L), but free T₄ (1.14 ng/dL, reference range 0.85-1.86 ng/dL) and T₃ (1.20 ng/mL, reference range 0.78-1.82 ng/mL) levels were within the normal range. Serum cortisol (5.41 µg/dL, reference range 1.81-12.67 µg/dL), 17 α -OH progesterone (4 ng/dL, reference range \leq 20 ng/dL), and adrenocorticotrophic hormone (ACTH, 33.89 pg/mL, reference range 6.00-56.70 pg/mL) levels were also normal. To rule out PHP, further evaluations were performed. Ultrasonography and a scan (Tc-99m) of the thyroid and parathyroid glands were performed, but no abnormal findings were found. There was no evidence of AHO features in either the hand X-rays or physical examination of the patient. However, computed tomography (CT) scan of the brain revealed multiple high-density nodular lesions in the bilateral basal ganglia and subcortical white matter of the frontal lobe (Fig. 2). The cAMP level in the 24-hr urine sample was slightly decreased (1.60 µmol/day, reference range 1.8-6.3 µmol/day).

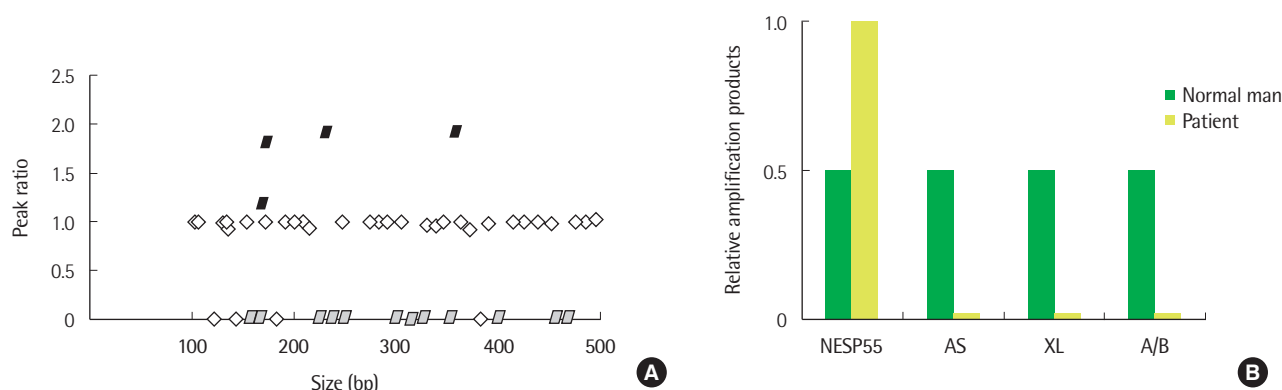


Fig. 3. MS-MLPA analysis of *GNAS* and *STX16*. (A) MS-MLPA peak ratio of patient treated after HhaI enzyme. Peaks for NESP55 (black colored box ■) and AS, XL, A/B (grey colored box ■) are expressed. (B) Relative copy numbers of DMRs (NESP55, AS, XL, and A/B) after HhaI restriction enzyme treatment to the each allele compared to healthy control. NESP55 conserved about a pair of alleles, suggesting gain of methylation in the paternal allele. AS, XL and AS showed a 100% reduction of relative peaks, suggesting that loss of methylations in the maternal allele.

2. Genetic Evaluation

First, we performed direct sequencing of *GNAS* and *STX16*. Amplification of exons was performed using primers designed to anneal sequences in the pre- and post-exon introns. PCR products were bidirectionally sequenced with the Big-Dye Terminator v3.1 Cycle Sequencing Kit (Applied Biosystems, Foster City, CA, USA) using the ABI PRISM 3130xl Genetic Analyzer (Applied Biosystems). The Sequencer program (GeneCodes Corp., Ann Arbor, MI, USA) was used to align the derived and reference sequences (NM_000516.4). In the direct sequencing of *GNAS* and *STX16*, no pathogenic mutations were detected.

A multiplex ligation-dependent probe amplification (MLPA) assay was performed to identify the presence of deletions and duplications, including DMRs, in the *GNAS* complex and *STX16*. Methylation-specific-MLPA (MS-MLPA) was performed to identify any abnormal methylation of the sequence and copy-number changes within the *GNAS* complex and *STX16*. MLPA and MS-MLPA were performed using the SALSA MS-MLPA probemix ME031-B1 *GNAS* kit (MRC-Holland, Amsterdam, The Netherlands) according to the manufacturer's protocol. The ME031-B1 probemix contains 25 probes specific for the *GNAS* locus and six probes specific for *STX16* with amplicon sizes between 125 and 500 nucleotides. DNA was denatured at 98°C for 5 min and hybridized with the probe set overnight at 60°C. The ligation reaction using ligase was performed for 30 min at 48°C, followed by 5 min at 98°C for heat inactivation of the enzyme. PCR was performed with the specific SALSA PCR primers for 35 cycles (95°C for 30 sec; 60°C for 30 sec; 72°C for 1 min). MLPA fragment analysis data was generated using the Applied

Biosystems 3130xl Genetic Analyzer and analyzed using GeneMarker software (SoftGenetics, State College, PA, USA). A sample from a healthy male was used as the normal control in both MLPA and MS-MLPA assays.

The results of the MLPA analysis revealed a normal copy number for both the *GNAS* complex and *STX16*. For the MS-MLPA assay, the restriction enzyme HhaI was used to assess methylation status within a given sample. Un-methylated DNAs were digested by HhaI, and the digested probes, not amplified by PCR, did not generate a signal. In the MS-MLPA, the control sample showed a 50% reduction of each DMR (NESP55, NESPAS, XL, A/B domains), which is consistent with the previously reported normal methylation pattern (Fig. 3). In the patient's sample, the NESP55 peak was 100% preserved, but peaks of NESPAS, XL, and A/B domains showed a 100% reduction, compared to those in the non-HhaI treated sample. This suggests gain of methylation in the NESP55 domain and loss of methylation in the NESPAS, XL, and A/B domains of the maternal allele.

DISCUSSION

PHP presents different disease features according to its subtypes owing to genetic and epigenetic aberrations in the *GNAS* complex [1, 3]. The *GNAS* complex, a highly imprinted region, provides a better understanding of the pathogenesis of this disease. PHP-Ia and PHP-Ib are caused by distinct mechanisms, but some clinically overlapping cases have been reported [8]. In cases with an uncertain diagnosis, careful clinical examination, including as-

assessment of AHO-specific manifestations and further laboratory and radiological investigations, are needed. Blood biochemical parameters and urinary calcium excretion should be monitored in patients with PHP-I. In case of children, height, growth velocity, and pubertal development should be closely observed. High birth weight and/or early-onset obesity and macrocephaly are features of paternal uniparental disomy (UPD) of chromosome 20q. The most sporadic cases of PHP-Ib demonstrate broad *GNAS* methylation defects, and no specific gene mutation has been identified as a cause of the methylation defects. Some cases of PHP-Ib have been identified to have paternal UPD as the underlying cause (10-25% according to various reports) [16, 18, 19].

In Korea, several cases of PHP-Ib have been previously reported [20]. Cho et al. described six patients with PHP-Ib exhibiting various symptoms at diagnosis, such as seizures or carpal spasm. Two of the patients with PHP-Ib also showed intracranial calcifications that were revealed by a brain CT scan. Molecular studies also revealed methylation defects of the *GNAS* DMRs and *STX16* deletions in the patients with PHP-Ib. Cho et al. suggested a diagnostic progression of direct sequencing of the *GNAS* gene followed by MS-MLPA of both *GNAS* DMRs and *STX16* for the diagnosis of patients without AHO features. Microsatellite analyses were recommended to exclude paternal disomy if parental DNA was available. Garin et al. recommended single CpG bisulphite-based methods to confirm the results in patients with partial methylation defects [19]. A pyrosequencing method with bisulphite treatment is useful for the detection of more subtle methylation defects. However, MS-MLPA has the advantage of providing quantification of methylation along with detection of gene deletions and duplications. MS-MLPA analysis consists of two parts—determining copy numbers by comparing different undigested samples, and determining methylation patterns by comparing each undigested sample to its digested counterpart. The second part is unique to MS-MLPA probe mixes and serves to semi-quantify the percentage of methylation within the given sample. In our case, we performed simultaneous direct sequencing of *GNAS* and *STX16* because the patient had no familial history and had ambiguous clinical features, such as high-density lesions revealed by a brain CT scan. After direct sequencing, MS-MLPA was performed, but without parental DNA owing to its unavailability. In previously reported Korean cases of PHP-Ib and in our case, the most frequent aberrant methylation pattern was gain of methylation in the NESP55 domain and

loss of methylation in the NESPAS, XL, and A/B domains. The cases of PHP are not sufficient to prepare an appropriate diagnostic workflow; it only allows us to ascertain the origin of the disease and provides the evidence for further genetic counseling. Each study presents a different work-flow in use for PHP diagnosis, but all studies emphasize the use of MS-MLPA. In our case, the patients showed elevated TSH levels and normal free T4 and T3 levels. TSH resistance is frequently noted in patients with PHP-Ia, while less commonly in patients with PHP-Ib. Compared to previously reported Korean cases of PHP-Ib [20], our case showed significantly low PTH levels (127 mmol/L vs. 306.3 ± 119.1 mmol/L, $P=0.014$) and relatively high TSH levels (8.42 mIU/L vs. 5.75 ± 5.71 mIU/L, $P=0.3$). Intracranial calcification can be observed in both subtypes. Overlapping laboratory and physical findings in PHP subtypes have made differential diagnosis challenging. Nonetheless, molecular analyses are reliable methods for PHP diagnosis. In conclusion, in addition to the *GNAS* and *STX16* analyses using direct sequencing, quantitative analysis of gene copy number and detection of methylation defects are required for the diagnosis of PHP. Thus, MS-MLPA is a suitable method for identifying and understanding the disease.

AUTHORS' DISCLOSURE OF POTENTIAL CONFLICTS OF INTEREST

No potential conflicts of interest relevant to this article were reported.

ACKNOWLEDGMENTS

We would like to thank all patients who participated in this study, the referring clinicians, and The Catholic Genetic Laboratory Center for assisting us with this study. This study was supported by Research Fund of Seoul St.Mary's Hospital, The Catholic University of Korea.

REFERENCES

1. Mantovani G. Clinical review: Pseudohypoparathyroidism: diagnosis and treatment. *J Clin Endocrinol Metab* 2011;96:3020-30.
2. Drezner M, Neelon FA, Lebovitz HE. Pseudohypoparathyroidism type II: a possible defect in the reception of the cyclic AMP signal. *N Engl J*

- Med 1973;289:1056-60.
3. Bastepe M. The *GNAS* Locus: Quintessential complex gene encoding Galpha, XLalphas, and other imprinted transcripts. *Curr Genomics* 2007;8:398-414.
 4. Yuno A, Usui T, Yambe Y, Higashi K, Uqi S, Shinoda J, et al. Genetic and epigenetic states of the *GNAS* complex in pseudohypoparathyroidism type 1b using methylation-specific multiplex ligation-dependent probe amplification assay. *Eur J Endocrinol* 2013;168:169-75.
 5. Bastepe M, Fröhlich LF, Hendy GN, Indridason OS, Josse RG, Koshiyama H, et al. Autosomal dominant pseudohypoparathyroidism type 1b is associated with a heterozygous microdeletion that likely disrupts a putative imprinting control element of *GNAS*. *J Clin Invest* 2003;112:1255-63.
 6. Linglart A, Bastepe M, Jüppner H. Similar clinical and laboratory findings in patients with symptomatic autosomal dominant and sporadic pseudohypoparathyroidism type 1b despite different epigenetic changes at the *GNAS* locus. *Clin Endocrinol* 2007;67:822-31.
 7. Liu J, Nealon JG, Weinstein LS. Distinct patterns of abnormal *GNAS* imprinting in familial and sporadic pseudohypoparathyroidism type 1b. *Hum Mol Genet* 2005;14:95-102.
 8. Mantovani G, Bondioni S, Linglart A, Maghnie M, Cisternino M, Corbetta S, et al. Genetic analysis and evaluation of resistance to thyrotropin and growth hormone-releasing hormone in pseudohypoparathyroidism type 1b. *J Clin Endocrinol Metab* 2007;92:3738-42.
 9. Bastepe M, Pincus JE, Sugimoto T, Tojo K, Kanatani M, Azuma Y, et al. Positional dissociation between the genetic mutation responsible for pseudohypoparathyroidism type 1b and the associated methylation defect at exon A/B: evidence for a long-range regulatory element within the imprinted *GNAS1* locus. *Hum Mol Genet* 2001;10:1231-41.
 10. Liu J, Litman D, Rosenberg MJ, Yu S, Biesecker LG, Weinstein LS. A *GNAS1* imprinting defect in pseudohypoparathyroidism type 1b. *J Clin Invest* 2000;106:1167-74.
 11. Linglart A, Bastepe M, Jüppner H. Similar clinical and laboratory findings in patients with symptomatic autosomal dominant and sporadic pseudohypoparathyroidism type 1b despite different epigenetic changes at the *GNAS* locus. *Clin Endocrinol* 2007;67:822-31.
 12. Kidd GS, Schaaf M, Adler RA, Lassman MN, Wray HL. Skeletal responsiveness in pseudohypoparathyroidism: a spectrum of clinical disease. *Am J Med* 1980;68:772-81.
 13. Murray TM, Rao LG, Wong MM, Waddell JP, McBroom R, Tam CS, et al. Pseudohypoparathyroidism with osteitis fibrosa cystica: direct demonstration of skeletal responsiveness to parathyroid hormone in cells cultured from bone. *J Bone Miner Res* 1993;8:83-91.
 14. Balkissoon AR, Hayes CW. Case 14: intramedullary osteosclerosis. *Radiology* 1999;212:708-10.
 15. Sbrocchi AM, Rauch F, Lawson ML, Hadjiyannakis S, Lawrence S, Bastepe M, et al. Osteosclerosis in two brothers with autosomal dominant pseudohypoparathyroidism type 1b: bone histomorphometric analysis. *Eur J Endocrinol* 2011;164:295-301.
 16. Bastepe M, Altug-Teber O, Agarwal C, Oberfield SE, Bonin M, Jüppner H. Paternal uniparental isodisomy of the entire chromosome 20 as a molecular cause of pseudohypoparathyroidism type 1b (PHP-1b). *Bone* 2011;48:659-62.
 17. Bastepe M, Lane AH, Jüppner H. Paternal uniparental isodisomy of chromosome 20q--and the resulting changes in *GNAS1* methylation--as a plausible cause of pseudohypoparathyroidism. *Am J Hum Genet* 2001;68:1283-9.
 18. Dixit A, Chandler KE, Lever M, Poole RL, Bullman H, Mughal MZ, et al. Pseudohypoparathyroidism type 1b due to paternal uniparental disomy of chromosome 20q. *J Clin Endocrinol Metab* 2013;98:E103-8.
 19. Garin I, Mantovani G, Aguirre U, Barlier A, Brix B, Elli FM, et al. European guidance for the molecular diagnosis of pseudohypoparathyroidism not caused by point genetic variants at *GNAS*: an EQA study. *Eur J Hum Genet* 2015;23:438-44.
 20. Cho SY, Yoon YA, Ki CS, Huh HJ, Yoo HW, Lee BH, et al. Clinical characterization and molecular classification of 12 Korean patients with pseudohypoparathyroidism and pseudopseudohypoparathyroidism. *Exp Clin Endocrinol Diabete* 2013;121:539-45.